

The effects of randomly occurring nonuniformities on propagation in photonic crystal fibers

Kristen Lantz Reichenbach and Chris Xu

School of Applied and Engineering Physics, Cornell University, Ithaca, NY 14853
KPL22@cornell.edu

Abstract: The effects of random imperfections in the lattice of a photonic crystal fiber on the propagation of the fundamental mode are analyzed using numerical simulations based on the multipole method. Lattice irregularities are shown to induce significant birefringence in fibers with large air holes but to cause a negligible increase in the confinement loss for low loss fibers. The dispersion is shown to be robust if the percentage of variation in the fiber parameters is less than 2% and the structure does not fall within a cutoff region. The coupling behavior in two-core structures with large air holes demonstrates high sensitivity to fiber nonuniformities. Understanding the discrepancies between the properties of simulated and fabricated fibers is an important step in leveraging the unique properties of PCFs.

©2005 Optical Society of America

OCIS codes: (060.2400) Fiber properties; (060.2270) Fiber characterization; (060.2280) Fiber design and fabrication

References and links

1. T. A. Birks, J. C. Knight and P. S. J. Russell, "Endlessly single-moded photonic crystal fiber," *Opt. Lett.* **22**, 961-963 (1997).
2. Boris T. Kuhlmeiy, "Theoretical and numerical investigation of the physics of microstructured optical fibres," Ph.D. thesis, University of Sydney, Australia. June 2004, <http://www.physics.usyd.edu.au/~borisk/physics/thesis.pdf>
3. P. Russell, "Photonic Crystal Fibers," *Science* **299**, 358-362 (2003).
4. T. M. Monro, P. J. Bennett, N. G. R. Broderick and D. J. Richardson, "Holey fibers with random cladding distributions," *Opt. Lett.* **25**, 206-208 (2000).
5. S. B. Libori, J. Broeng, E. Knudsen, A. Bjarklev and H. R. Simonsen, "High-birefringent photonic crystal fiber," in *Optical Fiber Communication Conference and Exhibit*, 2001. OFC 2001, Vol. 2 of OSA Proceedings Series (Optical Society of America, Washington, D.C., 1900), pp. TuM2-1-TuM2-3.
6. A. Cucinotta, S. Selleri, L. Vincetti and M. Zoboli, "Perturbation analysis of dispersion properties in photonic crystal fibers through the finite element method," *J. Lightwave Technol.* **20**, 1433-1442 (2002).
7. J. M. Fini, "Perturbative numerical modeling of microstructure fibers," *Opt. Express* **12**, 4535-4545 (2004), <http://www.opticsexpress.org/abstract.cfm?URI=OPEX-12-19-4535>.
8. I. K. Hwang, Y. J. Lee, Y. H. Lee, "Birefringence induced by irregular structure in photonic crystal fiber," *Opt. Express* **11**, 2799-2806 (2003), <http://www.opticsexpress.org/abstract.cfm?URI=OPEX-11-22-2799>.
9. K. Saitoh, Y. Sato and M. Koshiba, "Coupling characteristics of dual-core photonic crystal fiber couplers," *Opt. Express* **11**, 3188-3195 (2003). <http://www.opticsexpress.org/abstract.cfm?URI=OPEX-11-24-3188>.
10. L. Zhang and C. Yang, "Polarization splitter based on photonic crystal fibers," *Opt. Express* **11**, 1015-1020 (2003). <http://www.opticsexpress.org/abstract.cfm?URI=OPEX-11-9-1015>.
11. T. P. White, B. T. Kuhlmeiy, R. C. McPhedran, D. Maystre, G. Renversez, C. M. d. Sterke and L. C. Botten, "Multipole method for microstructured optical fibers. I. Formulation," *J. Opt. Soc. Am. B* **19**, 2322-2330 (2002).
12. B. T. Kuhlmeiy, T. P. White, G. Renversez, D. Maystre, L. C. Botten, C. M. d. Sterke and R. C. McPhedran, "Multipole method for microstructured optical fibers. II. Implementation and results," *J. Opt. Soc. Am. B* **19**, 2331-2340 (2002).
13. CUDOS MOF UTILITIES Software ©Commonwealth of Australia 2004. All rights reserved. <http://www.physics.usyd.edu.au/cudos/mofsoftware/>.
14. G. P. Agrawal, *Nonlinear Fiber Optics*, 3rd ed. (Academic Press, San Diego, CA, 2001), pg. 8.

15. M. J. Steel, T. P. White, C. M. de Sterke, R. C. McPhedran and L. C. Botten, "Symmetry and degeneracy in microstructured optical fibers," *Opt. Lett.* **26**, 488-490 (2001).
 16. B. T. Kuhlmeiy, R. C. McPhedran, C. M. de Sterke, P. A. Robinson, G. Renversez, and D. Maystre, "Microstructured optical fibers: where's the edge?," *Opt. Express* **10**, 1285-1290 (2002), <http://www.opticsexpress.org/abstract.cfm?URI=OPEX-10-22-1285>.
 17. N. I. Nikolov, T. Srensen, O. Bang and A. Bjarklev, "Improving efficiency of supercontinuum generation in photonic crystal fibers by direct degenerate four-wave mixing," *J. Opt. Soc. Am. B* **20**, 2329-2337 (2003).
 18. W. E. P. Padden, M. A. v. Eijkelenborg, A. Argyros and N. A. Issa, "Coupling in a twin-core microstructured polymer optical fiber," *Appl. Phys. Lett.* **84**, 1689-1691 (2004).
-

1. Introduction

Photonic crystal fibers (PCFs) have received significant attention from the scientific community due to their unique propagation characteristics [1-3]. The cross-section of a PCF consists of a periodic lattice of dielectric materials, typically a solid silica material permeated by air holes arranged in a triangular lattice, and extends parallel to the fiber axis. Propagation is achieved through the creation of a defect in the periodic lattice. This defect can be of lower index than the average index of the cladding, typically resulting from a large central air hole, which leads to photonic band gap propagation. For the type of PCFs studied in this paper, however, light propagates by means of modified total internal reflection, which occurs when the central defect is a silica core. Because the core has a higher index than the average index of the cladding, these PCFs can be compared to conventional step index fibers with a wavelength dependent cladding index. This important distinction when assigning a value to the cladding index explains the endlessly single mode behavior observed in PCFs with small air holes [1].

The use of PCFs for both system and device level applications sometimes requires novel hole arrangements. Because of the cost and effort necessary for the fabrication of PCFs, precise numerical simulations are essential to guide the design process. A variety of numerical modeling methods are currently available that accurately calculate PCF properties; however, it is fastest and easiest to simulate perfect structures that have precisely located, exactly circular, air holes. Random variations in the photonic crystal lattice are inherent to the fabrication of PCFs and complicate the validity of predictions based on perfect fibers since fiber parameters can only be guaranteed with limited precision. The degree to which these structural non-uniformities affect the propagation of the fundamental mode has not been completely understood. Awareness of the sensitivity different fiber properties have to lattice imperfections and the degree of structural variations that can be tolerated will be helpful tools for future PCF designs.

Previous studies that have been performed in this area focus predominantly on calculating the birefringence induced from reduced symmetry in the lattice of a PCF [4-8]. The structural variations analyzed are typically not random in nature [5, 6] and therefore do not accurately represent those that result from fabrication. Practical laboratory or industrial use of PCFs for single-mode transmission, dispersion compensation, or white light generation necessitates an understanding of the birefringence as well as the loss and dispersion properties of the fabricated fibers. Multiple core PCF devices such as filters, couplers, and polarization splitters [9, 10] depend on the predictability of coupling behavior between cores. Therefore, in this paper, we study the effect of stochastic variations in a PCF cross-section on the birefringence, the confinement loss, and the dispersion of a single core PCF and on the coupling length of a two-core PCF.

2. Method

Numerical simulations based on the multipole method, as applied to PCFs by White et al. and Kuhlmeiy et al. [11, 12], are used to determine the mode effective indices of the PCF structures studied. The presented results are a combination of data from a program written by

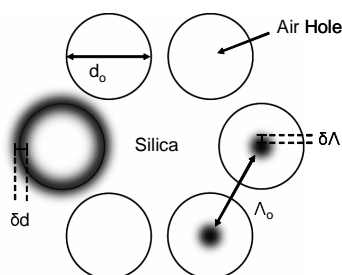


Fig. 1. An example of the geometry analyzed including definitions of important parameters and variations.

the author and from the CUDOS MOF UTILITIES Software created and distributed by the University of Sydney [13]. The accuracy of the programs has been assessed according to the recommended methods in ref. 12. The precision of the calculated mode indices is at least $1e-11$ for the real part [13] and the precision for the imaginary part of the index is $1e-15$ [2, 12]. Because the smallest index differences examined in this paper are on the order of $1e-6$, we are confident about the numerical precision of our modeling tool.

The fibers simulated are composed of air holes arranged in a triangular lattice and centered around a silica defect where the light is guided. The structure of a PCF is completely described by two parameters: the air hole diameter, d , and the air hole separation or pitch, Λ . The effects of variations in the air hole size (d) and in the location of the air holes (Λ) are analyzed separately by generating a Gaussian distribution of random values for d or Λ with standard deviations δd or $\delta \Lambda$ and mean values d_0 or Λ_0 . Each air hole in the fiber cross-section is independently assigned a value for the given parameter from the distribution in order to create one test fiber. An illustration of these terms and variations appears in Fig. 1. As shown in the figure, variations in Λ are two dimensional, therefore random in both magnitude and direction. Fiber non-uniformities are quantified through the definition of a percentage of variation as the ratio of the standard deviation to the mean of the distribution (ie. $\delta d/d_0$ or $\delta \Lambda/\Lambda_0$) times 100. The range of percentages was chosen to practically represent the degree of irregularity in current PCFs.

The wavelength of light is $1.55 \mu\text{m}$ unless otherwise stated and the index of refraction of silica is determined according to the Sellmeier equation [14]. A minimum number of air holes are simulated without sacrificing accuracy in order to maintain manageable computation times.

3. Results and discussion

3.1 Birefringence

Theoretical calculations based on group theory have shown that fibers with six fold rotational symmetry, like the standard triangular lattice PCF, will never show splitting in the fundamental mode [15]. Small imperfections in the photonic crystal lattice that are produced during the fabrication process, however, create asymmetries that break the degeneracy and lead to birefringence. The birefringence, defined as the difference in the index of the x and the y polarized modes, was calculated for the fundamental mode of fibers with randomly generated structural variations and the results appear in Fig. 2. The average value for the pitch was chosen to be $\Lambda_0 = 2.5 \mu\text{m}$ for two different air hole sizes: $d_0 = 2.25 \mu\text{m}$ and $d_0 = 1.75 \mu\text{m}$. An image of the energy distribution of the fundamental mode of each fiber is inset in Fig. 2. The marker indicates the average value for the birefringence of thirty random structures with each type of variation at each percentage variation, while the bars represent the spread or standard deviation of the data set. The dotted lines demonstrate a linear

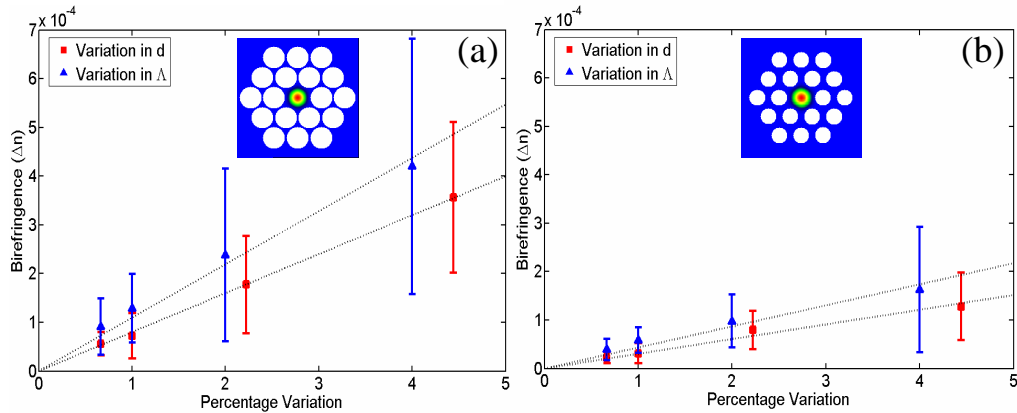


Fig. 2. The calculated birefringence for two different fibers with $\Lambda_0 = 2.5 \mu\text{m}$ and $\lambda = 1.55 \mu\text{m}$: (a) $d_0/\Lambda_0 = 0.90$ and (b) $d_0/\Lambda_0 = 0.70$. Markers indicate the average birefringence for a data set of 30 random structures for each percentage variation and each type of variation, while the bars represent the spread or standard deviation. The fit is linear. Insets display the fundamental mode for the fibers calculated.

relationship between the induced birefringence and the percentage variation, therefore supporting earlier results obtained in numerical simulations using the plane wave expansion method [8]. With the data presented here, these conclusions are extended to fibers with much larger air holes. For the two air hole sizes studied, we found that fibers with larger air holes experience a greater induced birefringence than fibers with smaller air holes (Fig. 2). In fact, the values for the birefringence appearing in Fig. 2 are more than an order of magnitude larger than the values calculated by Ref. [8] for fibers with even smaller air holes ($d/\Lambda = 0.46$ and $\lambda/\Lambda = 0.48$) and the same degree of lattice nonuniformity [8]. As shown in Fig. 2(a), birefringence comparable to standard polarization maintaining fibers can be induced from a relatively low degree of random structural nonuniformity in PCFs with air holes that are large relative to the pitch.

3.2 Confinement loss

Due to the finite nature of the photonic crystal lattice in PCFs, all modes are leaky and the resulting confinement loss can be calculated from the imaginary part of the mode index using Eq. (1):

$$\text{Loss}(dB/km) = \frac{20}{\ln(10)} \frac{2\pi}{\lambda} \Im(n_{\text{eff}}) \times 10^9, \quad (1)$$

where λ is the wavelength in units of μm and n_{eff} is the effective mode index. Loss calculations were performed on a PCF with average parameter values of $\Lambda_0 = 2.5 \mu\text{m}$ and $d_0 = 2.25 \mu\text{m}$, therefore $d_0/\Lambda_0 = 0.90$. In Fig. 3, the markers represent the calculated loss for thirty randomly generated structures with each type of variation for each percentage variation. Although the average loss as well as the spread in the loss values increase with the degree of random imperfections in the fiber structure, the loss remains much below the actual loss of current PCFs, which is dominated by Rayleigh scattering and IR absorption for index guiding PCFs. Similar results were also found for a different fiber with smaller air holes. Thus, the impact of the imposed structural irregularities on the actual propagation loss is inconsequential for PCFs with low confinement loss.

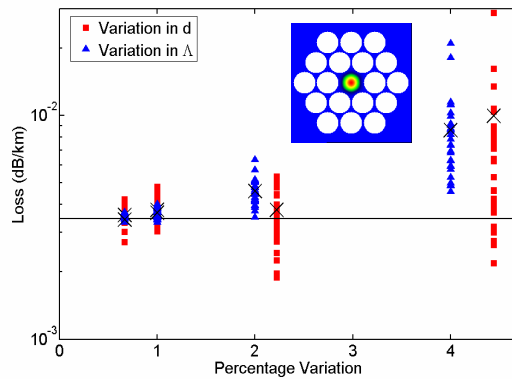


Fig. 3. Loss plotted versus the percentage variation; the solid line is the predicted loss for the structure with a perfect lattice. The markers represent the values for the loss calculated from 30 random structures for each percentage variation and type of variation. The X indicates the average loss for the data set. Inset is an image of the fundamental mode of the fiber with $\Lambda_0 = 2.5 \mu\text{m}$ and $d_0 = 2.25 \mu\text{m}$, $\lambda = 1.55 \mu\text{m}$.

3.3 Dispersion

The design of PCFs demonstrating novel dispersion properties, such as ultra-flattened dispersion and anomalous dispersion at shorter wavelengths than $1.3 \mu\text{m}$, relies on the accuracy of numerical simulations for predicting these behaviors and for easily testing new ideas. PCFs characterized by dispersion properties that cannot be exhibited by conventional fibers, such as ultra-flattened or oscillating dispersion, tend to fall within a cutoff region [2, 16]. This region is defined by the transition the mode-field area (MFA) experiences as the wavelength increases and the mode changes from being well confined with low loss to a high loss, space filling mode [2, 16]. PCFs whose dimensions fall within this region are also predicted to be extremely sensitive to lattice imperfections [2, 16]. We calculated the dispersion for a standard single core PCF with the average parameters $\Lambda_0 = 0.8 \mu\text{m}$ and $d_0 = 0.56 \mu\text{m}$, therefore $d_0/\Lambda_0 = 0.70$, over a wavelength range of $0.4 \mu\text{m}$ to $1.7 \mu\text{m}$. The dimensions of this PCF and the span of wavelengths cross the cutoff region. The dispersion is calculated from the second derivative of the mode index with respect to wavelength using Eq. (2):

$$D = \frac{-\lambda}{c} \frac{\partial^2 n_{eff}}{\partial \lambda^2} \quad (2)$$

The results appear in Fig. 4, where the markers represent the calculated zero dispersion wavelengths (ZDWs) for thirty randomly generated structures with each type of variation for each percentage variation. At the shorter ZDW, a percentage variation in the fiber parameters of about 4% or less will lead to a calculated ZDW within approximately $\pm 20 \text{ nm}$ of the predicted value from a perfect lattice. Near the second ZDW, the MFA has increased as the mode becomes less well confined and variations less than 2% are required in order to attain the same amount of certainty in the ZDW. Over the entire wavelength range examined, the MFA increases by a factor of three and the spread in calculated values for the dispersion as a function of wavelength increases dramatically but then begins to decrease again when leaving the cutoff region. These results support the existence of a cutoff region where structural variations have a significant impact on the dispersion.

PCFs with large air holes can be designed specifically for use in supercontinuum (SC) generation where high effective nonlinearities are required. For a wavelength range of $0.5 \mu\text{m}$ to $1.6 \mu\text{m}$, we calculated the dispersion of a typical highly nonlinear fiber (HNLF) with

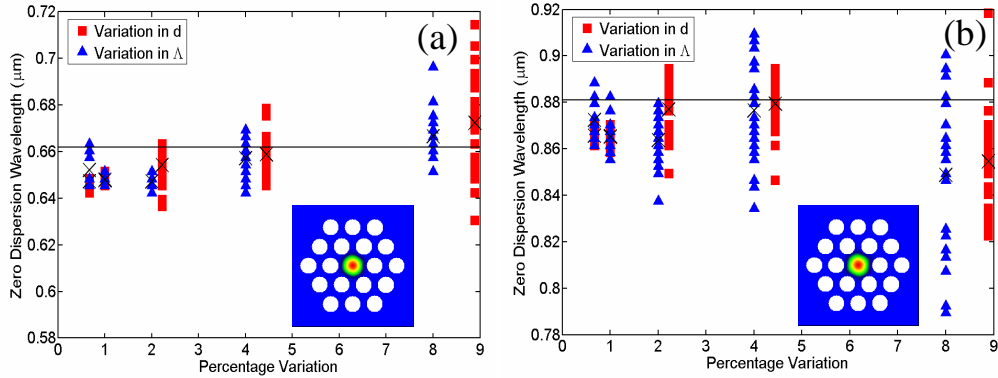


Fig. 4. The two zero dispersion wavelengths for a fiber with $d_0/\Lambda_0 = 0.70$ and $\Lambda_0 = 0.8 \mu\text{m}$ are plotted versus percentage variation. The markers indicate the values calculated for 30 randomly generated structures for each percentage variation and for two types of variations. The X represents the mean of the data and the solid line indicates the value for the perfect structure. The insets display the fundamental mode for the fiber at the respective wavelength.

$\Lambda_0 = 2.5 \mu\text{m}$ and $d_0 = 2.25 \mu\text{m}$, therefore $d_0/\Lambda_0 = 0.90$ (not falling in the cutoff region). A percentage variation of 2% or less resulted in an uncertainty in this structure's ZDW of about $\pm 4 \text{ nm}$. Since SC generation using direct degenerate four-wave mixing has been demonstrated through numerical simulations to be robust to variations in the ZDW of less than $\pm 3 \text{ nm}$ [17], variations of less than 2% are necessary for the HNLFF studied here. The MFA increases by a small amount ($\sim 25\%$) over the wavelength range examined and the uncertainty in the dispersion as a function of wavelength remains relatively constant, increasing only slightly. These calculations suggest that the dispersion properties of PCFs not falling in the cutoff region are relatively robust to small imperfections in the crystal lattice.

3.4 Two-core coupling

PCFs with two defects, or two-core PCFs, have been designed with unique air hole sizes and arrangements in order to customize the coupling properties between cores. Practical application of these concepts requires accurate predictions of the coupling, which may be

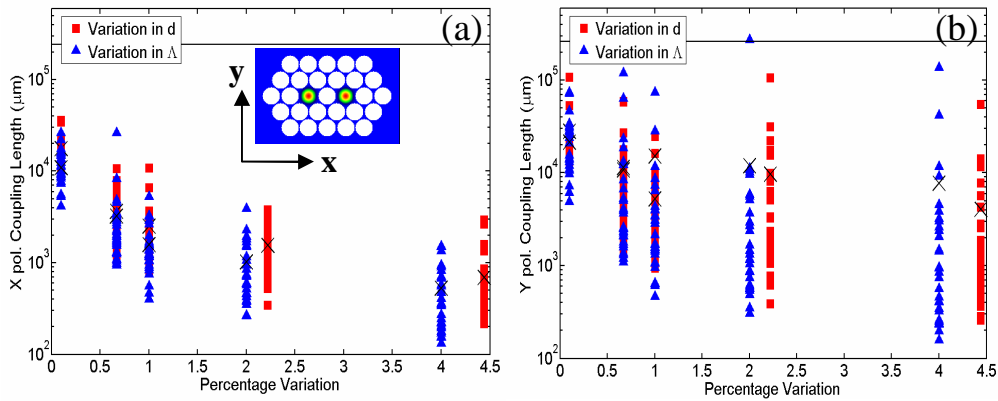


Fig. 5. The markers represent the calculated beat lengths for the x and y polarizations in (a) and (b), respectively; the X indicates the average for the data set. The solid lines are the predicted values for the structure with a perfect lattice. 30 random structures were simulated for each percentage variation for each type of variation. The inset in (a) displays the fundamental mode for the fiber calculated with $\Lambda_0 = 2.5 \mu\text{m}$ and $d_0 = 2.25 \mu\text{m}$, therefore $d_0/\Lambda_0 = 0.90$, and $\lambda = 1.55 \mu\text{m}$.

altered by unintentional imperfections in the fabricated fiber [18]. A key parameter for describing the coupling in a two-core structure is the beat length or coupling length. The fundamental mode of these fibers is split into four modes with slightly different indices and the coupling length is defined here as π divided by the difference in the propagation constants of modes with the same polarization. Figure 5(a) and 5(b) show the calculated values for the beat lengths of the x and y polarizations, respectively, for thirty randomly generated two-core fibers with variations in Λ and in d . The PCF parameters are $\Lambda_0 = 2.5 \mu\text{m}$ and $d_0 = 2.25 \mu\text{m}$, therefore $d_0/\Lambda_0 = 0.90$, and a reproduction of the fundamental mode of this fiber is inset in Fig. 5(a). The calculated beat lengths for the imperfect two-core PCFs differ from the predicted value (solid line) by up to two orders of magnitude even for very small degrees of variation and the spread in these values is quite large; consequently, even a slightly irregular crystalline structure significantly alters the mode propagation in this two-core structure and leads to a lack of certainty in the actual coupling properties of the fiber.

In order to isolate the characteristics of this fiber that make it so sensitive to lattice imperfections, we also calculated the beat lengths for two-core PCFs with smaller air holes but with the same average pitch. The results for these fibers appear in Fig. 6 and their parameters are as follows: $d_0 = 1.75 \mu\text{m}$, therefore $d_0/\Lambda_0 = 0.70$ (Figs. 6(a) and 6(b)); and $d_0 =$

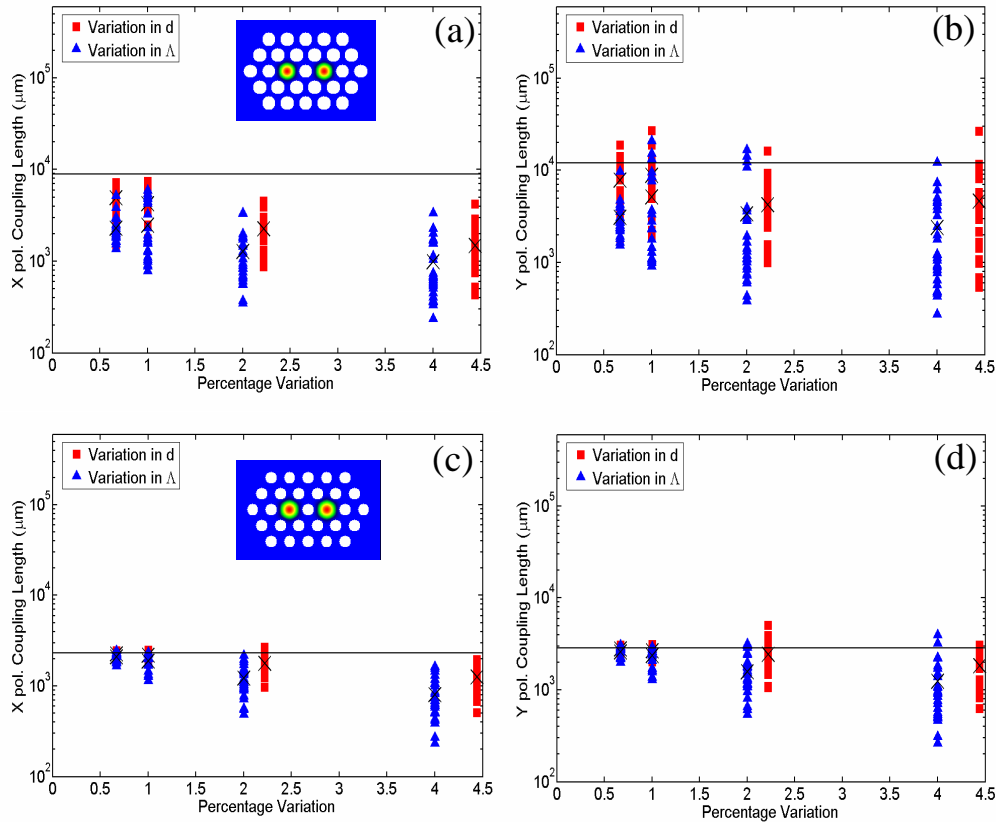


Fig. 6. The beat lengths for the x and y polarizations are plotted versus percentage variation for two fibers when $\lambda = 1.55 \mu\text{m}$: for (a) and (b), $d_0 = 1.75 \mu\text{m}$ and $d_0/\Lambda_0 = 0.70$, while for (c) and (d), $d_0 = 1.45 \mu\text{m}$ and $d_0/\Lambda_0 = 0.58$. The solid lines are the predicted values for the structure with a perfect lattice. The markers represent the calculated values for the coupling length while the X indicates the average for the data set; 30 random structures were simulated for each percentage variation for each type of variation. Insets display the fundamental mode for the fiber calculated.

Table 1. Summary of the fiber structures used in the two-core simulations

Λ_0	d_0	d_0/Λ_0	λ	MFA ^a	λ/Λ_0
2.5 μm	2.25 μm	0.90	1.55 μm	0.80	0.62
2.5 μm	1.75 μm	0.70	1.55 μm	1.13	0.62
2.5 μm	1.45 μm	0.58	1.55 μm	1.38	0.62

^a The mode-field area is normalized to the pitch of the structure squared and calculated from the z-component of the Poynting vector.

1.45 μm , therefore $d_0/\Lambda_0 = 0.58$ (Figs. 6(c) and 6(d)). See Table 1 for a summary of the parameters of the two-core fibers simulated. For both of these fibers, the properties of the fundamental mode, such as the MFA, the coupling, and the real part of the mode index, change insignificantly with the addition of a third ring of air holes, hence only two are used here in order to reduce computation time while maintaining accuracy. The smaller air holes found in these fibers reduce the index contrast between the air hole cladding and the core, resulting in a less confined mode with a larger area and therefore stronger coupling between the cores. The calculated values for the beat lengths in Fig. 6(c) and 6(d) are close to those of a perfect structure for percentage variations less than 2%. This fiber has the smallest air holes and is the least sensitive to lattice irregularities of the fibers studied, with the fiber in Fig. 5 experiencing the most effect. This behavior demonstrates that the air hole size and the coupling strength determine a two-core fiber's vulnerability to fabrication induced nonuniformities.

4. Conclusion

The susceptibility of a PCF to being fabricated with unintentionally high birefringence is strongly influenced by the air hole size of the fiber relative to the pitch, and birefringence comparable to polarization maintaining fibers can be induced from a relatively low percentage variation in the photonic crystal lattice when the air holes are large. For practical PCFs with very low confinement loss, the effect of lattice imperfections will not be discernable, although their impact on other types of loss, such as scattering, is unknown. The dispersion properties of PCFs are most susceptible to nonuniformities if the fiber falls within the cutoff region; however, outside of this region the fibers are more robust. For a typical HNLF, SC generation is predicted to tolerate variations in the fiber parameters of less than about 2% when the fiber is not within the cutoff region. Lastly, the coupling length has been shown to be very sensitive to perturbations in the lattice surrounding the defects when the air holes are large. Two-core fibers with smaller air holes and shorter coupling lengths are remarkably more robust. These results have strong implications for applications such as filters, couplers, and polarization splitters whose performance directly depends on the coupling properties of two or more cores.

Acknowledgments

The authors are grateful to Boris Kuhlmeier at the University of Sydney for exchange of emails concerning the use and understanding of his program and to John Fini at OFS Optics for

insightful discussions about the multipole method and programs based on this method. In addition, the authors acknowledge the University of Sydney through its ARC Centre of Excellence - Ultrahigh-bandwidth Devices for Optical Systems, School of Physics as the exclusive Licensor of the CUDOS MOF UTILITIES Software. This research was supported by the National Center for Research Resources (NCRR), National Institutes of Health.